Published in final edited form as:
Circulation. 2010 September 14; 122(11 0): S107–S117. doi:10.1161/CIRCULATIONAHA.109.930404.

Stromal Cell-Derived Factor-1α Activation of Tissue Engineered Endothelial Progenitor Cell Matrix Enhances Ventricular Function after Myocardial Infarction by Inducing Neovasculogenesis

John R. Frederick, M.D., **J. Raymond Fitzpatrick III, M.D.**, **Ryan C. McCormick, B.S.**, **David A. Harris, B.S.**, **Ah-Young Kim, M.S.**, **Jeffrey R. Muenzer, B.S.**, **Nicole Marotta, B.S.**, **Maximilian J. Smith, B.S.**, **Jeffrey E. Cohen, M.D.**, **William Hiesinger, M.D.**, **Pavan Atluri, M.D.**, and **Y. Joseph Woo, M.D.**
Division of Cardiovascular Surgery, Department of Surgery, University of Pennsylvania School of Medicine, Philadelphia, PA 19104

Abstract

Background—Myocardial ischemia causes cardiomyocyte death, adverse ventricular remodeling, and ventricular dysfunction. Endothelial progenitor cells (EPC) have been shown to ameliorate this process, particularly when activated with stromal cell-derived factor-1α (SDF). We hypothesized that implantation of a tissue engineered extracellular matrix scaffold seeded with EPCs primed with SDF could induce neovasculogenesis, prevent adverse remodeling, and preserve ventricular function after myocardial infarction (MI).

Methods and Results—Lewis rats (n=82) underwent left anterior descending artery ligation to induce MI. EPCs were cultured on a vitronectin/collagen scaffold, and primed with SDF to generate the activated EPC matrix (EPCM). EPCM was sutured to the anterolateral left ventricular (LV) wall including the region of ischemia.. At four weeks, when compared to controls, borderzone myocardial tissue demonstrated increased levels of VEGF in the EPCM group. Vessel density as assessed by immunohistochemical microscopy was significantly increased in the EPCM group (4.1 vs 6.2 vessels/high-powered field, $p<0.001$), and microvascular perfusion measured by lectin microangiography was enhanced four-fold (0.7 vs. 2.7% vessel volume/section volume, $p=0.04$). Ventricular geometry and scar fraction assessed by analysis of sectioned hearts exhibited significantly preserved LV internal diameter (9.7mm vs. 8.6mm, $p=0.005$) and decreased infarct scar expressed as percent of total section area (16% vs. 7%, $p=0.002$) when compared to all other groups. In addition, EPCM animals showed a significant preservation of function as measured by echocardiography, pressure volume-conductance, and Doppler flow.

Conclusions—Extracellular matrix seeded with EPCs primed with SDF induces borderzone neovasculogenesis, attenuates adverse ventricular remodeling, and preserves ventricular function after MI.

Corresponding Author: Y. Joseph Woo, M.D., 3400 Spruce St., 6 Silverstein, Philadelphia, PA 19104, Phone: 215-662-2956, Fax: 215-349-5798, wooy@uphs.upenn.edu.

Disclosures
None.

Keywords

Angiogenesis; Vasculogenesis; Endothelial Progenitor Cells; Extracellular Matrix; Ischemic Heart Disease

Background

The World Health Organization's *World Health Statistics 2008* report indicates that ischemic heart disease is on the rise and remains the most prevalent cause of death globally, constituting greater than 14% of all deaths.[1] Current therapies to combat ischemic cardiomyopathy include medical management, percutaneous coronary intervention, or coronary artery bypass grafting. The invasive strategies, however, are only applicable to patients with anatomically correctable atherosclerotic disease. A significant proportion of patients with coronary artery disease do not fall into this category, and many of these patients develop ischemic cardiomyopathy and fulminant heart failure refractory to medical management, for which the only amenable intervention is transplantation or ventricular assist devices used as destination therapy. The need for novel revascularization strategies is evident, and the emergence of cell therapy as a possible solution has prompted numerous investigations both in animal models[2] and more recently in human trials.[3–5]

Since the discovery of bone marrow-derived endothelial progenitor cells (EPC),[6] the concept of post-natal vasculogenesis, or neovasculogenesis, as a potential therapy for the sequelae of ischemic heart disease has been intensively investigated. These studies have employed a variety of delivery techniques including endogenous upregulation,[7–8] systemic delivery,[9] and local injection.[10] Many of these groups have shown a functional benefit of EPC therapy in the setting of myocardial ischemia, but few have been able to demonstrate a long-term effect. This is likely due to the high percentage of cell death and systemic dispersion that accompany both local and systemic injection. We propose that an extracellular matrix scaffold seeded with EPCs can overcome these limitations by providing a native environment in which the cells can thrive and enabling an insult-free delivery to the area of interest.

EPCs are thought to promote neovasculogenesis by two separate mechanisms. First, bone marrow-derived EPCs have been shown to incorporate themselves into newly formed vessels, crossing from the circulation into the interstitium in a manner similar to neutrophil adhesion and endothelial transmigration.[10–11] This strategy has been extensively studied, with most investigations focused on providing EPCs as the building blocks of new vessels, but translation of this therapy to human clinical trials has been plagued by the large number of cells needed to demonstrate a clinical benefit. In addition to the ability to form new vessels, EPCs are capable of eluting pro-angiogenic cytokines that induce new blood vessel growth by promoting the migration and proliferation of local endothelial cells.[12–14] Several groups have demonstrated a therapeutic benefit of administering these factors directly into the myocardium.[15] Known factors include but are not limited to vascular endothelial growth factor (VEGF) and stromal cell-derived factor-1α (SDF). Each of these factors plays a specific role in the angiogenic cascade. VEGF, for example, promotes endothelial cell

proliferation and subsequent angiogenesis,[16] while SDF functions as a chemotactic factor for the recruitment and activation of additional EPCs.[17]

We sought to develop a therapeutic strategy that amplifies the paracrine effects of EPCs. Previously, we have reported on the vasculogenic effects of SDF and endogenous EPC upregulation.[6–7] Additionally, our group has studied the functional benefits of extracellular matrix therapy with and without EPCs,[18–19] and other groups have shown promising results applying epicardial cell sheets for the treatment of ischemic cardiomyopathy.[20] We propose that combining these strategies by surgically implanting an EPC matrix which has been "supercharged" by pretreatment with SDF to serve as a myocardial "paracrine factory" will induce a robust neovasculogenic response. The aims of this study are to characterize the magnitude of the angiogenic response and to establish the functional benefit of a tissue engineered EPC matrix primed with SDF in the setting of myocardial ischemia. In order to further delineate the angiogenic and functional contribution of each component of our experimental model, we will also show data from additional experimental groups to demonstrate the superiority of activated EPC matrix therapy.

Methods

Cell isolation and generation of the EPC Matrix

Bone marrow mononuclear cells (MNC) were isolated from the long bones of syngeneic adult male Lewis rats (Charles River) by density-gradient centrifugation with Histopaque 1083 (Sigma) and seeded on the mucosal side of a decellularized porcine jejunal submucosa extracellular matrix (ECM). The seeded matrix was then cultured in Endothelial Basal Medium-2 supplemented with EGM-2 Singlequot (Lonza) containing hEGF, FBS, VEGF, hFGF-B, R3-IGF-1, ascorbic acid, heparin, gentamicin, and amphotericin-B. Seeded matrix is washed at day four to remove nonadherent cells. The combination of endothelial specific media and the inclusion of adherent cells is intended to select for the EPC phenotype. Prior to implantation on day seven, the matrix with or without cells is stimulated with SDF (R&D Systems) at a concentration of 100 ng/ml for 30 minutes in the respective SDF activated groups.

Immunohistochemical characterization of MNCs seeded on ECM

After seven days in endothelial specific media and the removal of nonadherent MNCs, the remaining cells which were adherent to the ECM were characterized by immunohistochemical analysis (n=5). Mouse anti-rat VEGFR2 (Novus Biologicals) was conjugated to biotin (Novus Biologicals, Lightning Link Kit). Cells adherent to the matrix were incubated with 4ug/ml Di-Iodinated acetyl-LDL (Invitrogen) at 37°C for 24 hrs and then washed three times with DPBS and incubated with 10ug/ml GSL I-isolectin B4 (Vector Laboratories, FL-1201) for 1hr. Cells were washed and blocked with 10% normal mouse serum (Abcam) for 10 min. 20uL/mL biotin conjugated mouse anti-rat VEGFR2 was added for 1hr followed by 8ul/mL Streptavidin-Allophycocyanin (BD Biosciences) for 45 min. Slides were washed and mounted using Vectashield with DAPI (Vector Laboratories). The cells were visualized via Confocal Microscopy (SCOPE MODEL) and images were

processed using ImageJ software (NIH). The EPC phenotype was defined as $DAPI^+$, Di-Iodinated acetyl-LDL^+, Isolectin-$B4^+$, and $VEGFR2^+$.

Characterization of isolated MNCs by flow cytometry

Mouse anti-rat VEGFR2 (Novus Biological) and rabbit anti-rat CXCR4 (Abcam) were conjugated to phycoerythrin (PE) and Atto 390, respectively (Novus Biologicals – Lightning Link Kits). Bone marrow mononuclear cells were harvested as stated above and non-specific binding was blocked with rabbit (10μg/ml) and mouse sera (10μg/ml) at room temperature for 10 minutes. Cells were stained with fluorescein isothiocyanate (FITC) conjugated mouse anti-rat CD3 (AdB Serotec), PE conjugated mouse anti-rat VEGFR2, Alexa Fluor 700 conjugated mouse anti-rat CD45 (AdB Serotec), and Atto 390 conjugated rabbit anti-rat CXCR4 (Abcam) at room temperature for 30 minutes. Viability was monitored by 7AAD nuclear stain (BD Biosciences). Fluorescence Minus Ones (FMOs) for each antibody, consisting of all antibodies but one, served as controls and defined negative populations for each stain. Cells were analyzed by a FACSCanto flow cytometer and data was analyzed using FloJo Software version 8.8.4 (TreeStar Inc.). EPCs were defined as the following phenotype in the lymphocyte population: $CD3^-$, $7AAD^-$, $CD45^+$, $VEGFR2^+$, $CXCR4^+$. FACS analysis was performed in triplicate.

Functional characterization of isolated MNCs cultured in endothelial specific media by Boyden Chamber Assay

Boyden chambers (Neuro Probe) were employed to assess EPC migration. Briefly, 8μm filters were loaded into control and experimental chambers. Eight day MNCs cultured in endothelial specific media on vitronectin coated plates were trypsinized, counted, and brought to a concentration of 90cells/μl in Dulbecco's phosphate buffered saline (DPBS). The bottom chamber of the control and experimental chambers were loaded with DPBS or 100ng/ml recombinant SDF (R&D systems) in, DPBS, respectively. A 560μl cell suspension was added to the top chamber of each. Both chambers were incubated at 37°C, 5%CO_2 for 4 hours. The cells remaining in the top chamber were wiped clean with a cotton swab and the filter was removed and mounted with Vectashield with DAPI (Vector Laboratories). Slides were visualized on a DF5000B Leica Fluorescent scope and analyzed via LASAF version 2.0.2 (Leica) software. Boyden chamber analysis was performed in triplicate.

Functional Characterization of Isolated MNCs Cultured in Endothelial Specific Media by Matrigel Assay

Growth Factor Reduced Matrigel (BD Biosciences) was thawed at 4°C and added to a 4-well chamber slide (500μl/chamber). The Matrigel was allowed to polymerize at 37°C, 5% CO_2 for 30 minutes. Fourteen day MNCs cultured in endothelial specific media on vitronectin coated plates were trypsinized and brought to a concentration of 100,000cells/ml in complete EBM-2 media, prepared as above. 500μl of the cell suspension was seeded onto the Matrigel-coated chambers and stored at 37°C, 5% CO_2 for 72 hours. Tubes were stained with Calcein AM (Molecular Probes) and visualized on a DF5000B Leica Fluorescent scope at 24, 48, and 72 hours. Matrigel assays were performed in triplicate.

Animal Care and Biosafety

Male Lewis rats weighing 250–300 g were obtained from Charles River. Food and water were provided ad lib. This investigation conforms with the *Guide for the Care and Use of Laboratory Animals* published by the US National Institutes of Health (NIH Publication No. 85-23, revised 1996) and was approved by the Institutional Animal Use and Care Committee of the University of Pennsylvania (Protocol #802076).

Ischemic Cardiomyopathy Model

Rats were anesthetized with ketamine (75 mg/kg) and xylazine (7.5 mg/kg), intubated with a 16-gauge catheter, and mechanically ventilated (Hallowell EMC) with a V_t (ml) = $6.2 \times M^{1.01}$ (M = animal mass, kg) and respiratory rate (min^{-1}) = $53.5 \times M^{-0.26.21}$ A thoracotomy was performed in the left fourth intercostal space, and a 7-0 polypropylene suture was placed around the mid-left anterior descending coronary artery (LAD) 2mm inferior to the left atrial appendage and ligated to produce a large anterolateral myocardial infarction of 30% of the left ventricle. The extent of infarction is highly reproducible in our hands and progression to cardiomyopathy has been well documented.[6–7,22–23] Following ligation, animals were randomly assigned to either the control (n=22) or one of four experimental groups consisting of the following: ECM alone (ECM, n=13), ECM stimulated with SDF (ECM+SDF, n=11), ECM seeded with cells but not activated with SDF (ECM+EPC, n=15), or ECM seeded with EPCs and activated with SDF (EPCM, n=21). In experimental animals, the matrix (0.75×0.75 cm^2) was sutured to the left ventricular anterolateral wall encompassing the area of ischemia. Control animals received a similar array of sutures with no matrix. The thoracotomy was closed and animals were implanted with identification microchips (BioMedic Data Systems Inc) and recovered. Buprenorphine (0.5mg/kg) was administered for postoperative analgesia. Identification data was maintained by an investigator who did not participate in subsequent data collection or analysis.

In Vivo Angiogenic Growth Factor Expression

To assess upregulation of angiogenic growth factors, hearts from a subset of animals (Control n=4, ECM+EPC n=4, EPCM n=5) were explanted 4 weeks following LAD ligation, and myocardial tissue biopsies were taken from the ischemic borderzone. Samples were homogenized in T-Per Tissue Extraction Reagent (Thermo-Fischer), normalized for total protein content via Quick Start Bradford Protein Assay (Bio-Rad Laboratories), and tested for presence of rat VEGF. Immunoblotting was performed using a mouse monoclonal antibody directed against rat VEGF (1:300, Abcam), and Horseradish peroxidase conjugated sheep anti-mouse IgG ECL secondary antibody (1:100,000, GE Healthcare). Chemiluminescent SuperSignal West Dura Extended Duration Substrate (Thermo Scientific) was used and images were captured using a ChemiDoc XRS+ system (Bio Rad). Assays were performed in triplicate.

In Vivo Inflammatory Analysis

To assess upregulation of inflammatory factors, hearts from a subset of animals (Control n=3, ECM+EPC n=3, EPCM n=3) were explanted 4 weeks following LAD ligation, and myocardial tissue biopsies were taken from the ischemic borderzone. Samples were

homogenized in T-Per Tissue Extraction Reagent (Thermo-Fischer), normalized for total protein content via Quick Start Bradford Protein Assay (Bio-Rad Laboratories), and tested for presence of rat tumor necrosis factor alpha (TNFα). Immunoblotting was performed using a rabbit polyclonal antibody directed against rat TNFα (1:100, Abcam), and Horseradish peroxidase conjugated sheep anti-rabbit IgG ECL secondary antibody (1:3000, GE Healthcare). Chemiluminescent SuperSignal West Dura Extended Duration Substrate (Thermo Scientific) was used and images were captured using a ChemiDoc XRS+ system (Bio Rad).

Assessment of Vessel Density

To assess microvascular angiogenesis, a subset of animals were sacrificed 4 weeks following LAD ligation (Control n=7, ECM n=5, ECM+SDF n=6, ECM+EPC n=7, EPCM n=6). Explanted hearts were distended with OCT compound (Sakura Finetek), submerged in an OCT-filled reservoir, frozen, and stored at −80°C. Transverse 10μm sections were prepared through the infarct level and co-stained with antibodies directed against platelet endothelial cell adhesion molecule (PECAM) and alpha smooth muscle actin (α-SMA). Sections were incubated with mouse anti-PECAM (1:500, BD Biosciences) and rabbit anti-α-SMA (1:500, Abcam) for 1 hour. Sections were then washed and incubated with Alexa Fluor 555 donkey anti-mouse IgG (1:500, Invitrogen) and Alexa Fluor 488 donkey anti-rabbit IgG (1:500, Invitrogen) for 1 hour. Slides were washed and mounted with Vectashield (Vector Laboratories). Quantitative analysis of vessels co-staining for PECAM and α-SMA was conducted with 40X fluorescent microscopy in the infarct zone, peri-infarct borderzone, and remote myocardium. Counts were conducted in a group-blinded fashion in 4 fields per specimen for each of the three zones and averaged.

Assessment of Microvascular Perfusion with Lectin Angiography

To ensure that newly formed microvessels are functionally perfused, a subset of animals (Control n=4, ECM+EPC n=3, EPCM n=3) underwent lectin microvascular angiography. 500 μg/kg of fluorescein-labeled *Lycopersicon esculentum* (tomato) lectin (Vector Laboratories) was injected into the IVC and circulated by the heart for 5 minutes. Direct contact of lectin with endothelial cells is required for binding to the surface N-acetylglucosamine oligomers of endothelial cells, so only perfused vessels are labeled.[24] Following lectin perfusion, hearts were explanted. Image stacks were obtained with scanning laser confocal microscopy through 100μm thick myocardial sections of infarct, borderzone, and remote myocardial regions. Three-dimensional reconstructions of the Z-stacks were created with Volocity Software v.3.61 (Improvision Inc). Flourescein-labeled voxels were quantified as a percentage of total tissue section voxels, creating a quantifiable measurement of perfusion per unit of myocardial tissue volume.

Infarct Size and Ventricular Geometry Analysis

Four weeks following LAD ligation, after myocardial functional analysis described below, a subset of animals' hearts were explanted (Control n=10, ECM n=5, ECM+EPC n=7, EPCM=7). The left and right ventricles were injected with OCT through the aorta and pulmonary artery respectively at standard pressures, and the heart was submerged in OCT,

frozen, and stored at −80°C. Each specimen was carefully oriented in an open OCT reservoir with the ligation sutures and external cardiac anatomy as a guide to ensure that each heart was positioned in exactly the same fashion. 10μm sections from midway between the apex and point of ligation were prepared and stained with hematoxylin and eosin (H&E). Using the papillary muscles as a landmark, two sections per animal were made perpendicular to the long axis of the left ventricle at its widest dimension approximately 200 microns basal to the muscles to ensure uniform comparisons between animals. Measurements were performed on digitized photomicrographs of the sections using Adobe Photoshop CS3 Extended v.10.0 image processing software (Adobe Systems Inc) with a standard of known length. Left ventricular internal diameter (LVID), borderzone wall thickness, infarct area, and cross-sectional area of the entire heart were recorded for each of the sections.

Echocardiographic Assessment of LV Geometry and Function

Left ventricular (LV) geometry and function were evaluated at 2 weeks (Control n=5, EPCM=4) and 4 weeks (Control n=22, EPCM n=21) following LAD ligation by transthoracic echocardiography utilizing a Phillips Sonos 5500 revD system (Phillips Medical Systems N.A.) with a 12-MHz transducer at an image depth of 2cm. Rats (Control n=22, Experimental n=21) were anesthetized and placed in the dorsal recumbency position. Left parasternal LV short axis 2-D and M-mode images were used to define LV anterolateral infarct wall thickness, LV internal diameters during systole and diastole, and fractional shortening.[25] All analyses were performed by a single investigator in a group blinded fashion.

Invasive Hemodynamic Assessment

Four weeks after LAD ligation, control and experimental animals (Control n=22, ECM n=10, ECM+EPC n=15, EPCM n=21) underwent invasive hemodynamic measurements with a pressure-volume (P-V) conductance catheter (SPR-869, Millar Instruments Inc). The catheter was calibrated via five point cuvette linear interpolation with parallel conductance subtraction by the hypertonic saline method.[21] Rats were anesthetized and the catheter was introduced into the LV with a closed-chest approach via the right carotid artery. Measurements were obtained before and during IVC occlusion to produce static and dynamic P-V loops under varying load conditions. Data were recorded and analyzed with LabChart v.6 software (AD Instruments) and ARIA Pressure Volume Analysis software (Millar Instruments).

In addition to P-V conductance catheter analysis, invasive cardiac output measurements were made by placing a Doppler flow probe (Transonics) around the ascending aorta after median sternotomy (Control n=20, EPCM n=16).

Statistical Analysis

The unpaired Student’s t-test was used to compare groups. Values are expressed as mean ± standard error of the mean (SEM). Statistical significance was defined by $P \leq 0.05$.

Results

Isolated MNCs Seeded on the ECM Show EPC Cell Markers after Seven Days in Endothelial Specific Media

At day seven in culture, isolated MNCs grown on extracellular matrix show universal expression of VEGFR2, stain positive for Isolectin, and show uptake of Di-Iodinated acetyl-LDL (Figure 1A), all of which are characteristic of EPCs. Scanning electron micrographs of ECM before (Figure 1B) and after (Figure 1C) seeding with EPCs show densely populated, adherent cells.

Isolated MNCs Express EPC Markers as Evidenced by Flow Cytometry

FACS analysis reveals a subpopulation of the mononuclear fraction (0.03% of total cells) which expresses VEGFR2, CD45, and CXC-R4; all of which are accepted EPC markers. This data indicates that EPCs are present in the isolated mononuclear cell fraction prior to culture.

Isolated MNCs Cultured in Endothelial Specific Media Exhibit Functional Characteristics of EPCs

Utilizing a Boyden chamber assay, 8 day cells show increased migration when placed in an SDF gradient (Control 105±5 cells/HPF vs. SDF 323±20 cells/HPF, p=0.006). Utilizing the Matrigel tube formation assay, 14 day cells show progressive sprout and tubule formation at 24 (Figure 2A), 48 (Figure 2B), and 72 hours (Figure 2C) and stain positive with Calcein AM (green), an endothelial marker. These data indicated that the isolated cells exhibit endothelial differentiation capacity consistent with EPCs.

In vivo Angiogenic Growth Factors Are Upregulated in the EPCM Group

At four weeks, immunoblotting revealed a distinct qualitative increase in rat VEGF expression in the EPCM animals versus the control and ECM+EPC groups. Representative immunoblot is shown in Figure 3.

In vivo Levels of Borderzone TNFα Are Not Statistically Different between Groups

At four weeks, immunoblotting revealed similar levels of TNFα between the control, ECM +EPC, and EPCM groups, as depicted in Figure 4. Quantitative analysis demonstrated intensities of 76.6 ± 1.4, 69.6 ± 0.7, and 75.2 ± 0.5 intensity units, respectively. Statistical comparisons revealed no statistically significant difference (control vs. ECM+EPC, P=0.24; control vs. EPCM, P=0.44, ECM+EPC vs. EPCM, P=0.16).

Borderzone Vessel Density Is Greatest in the EPCM Group

Analysis of immunofluorescent co-expression of PECAM and α-SMA revealed a significant increase in blood vessel density in the borderzone region of EPCM animals when compared to other groups. Quantitative analysis of vessel density showed 4.1 ± 0.3 vessels/high-powered field (HPF) in the control group (Figure 5A) compared to 6.2 ± 0.3 vessels/HPF in the treated group, P<0.001 (Figure 5B). Additional comparisons showed the following vessel densities: ECM+SDF 5.0 ± 0.3 vessels/HPF, ECM+EPC 5.5 ± 0.2 vessels/HPF.

When compared to the EPCM group, these values were significantly lower with P values of 0.006 and 0.03, respectively. Vessel density in remote myocardium was equivalent between EPCM (9.7 ± 0.3 vessels/HPF) and control animals (9.5 ± 0.5 vessels/HPF, P=0.7), and other groups exhibited similar results.

Borderzone Microvascular Perfusion Is Enhanced Following EPCM Treatment

Remote myocardial perfusion was equivalent between EPCM and control groups (4.3 ± 0.3% vessel volume/tissue volume vs. 3.8 ± 1.0%, P=0.7). This served as an internal control, validating the assay and demonstrating similar baseline perfusion in the two groups. Quantitative analysis demonstrated significantly enhanced perfusion in the borderzone region of EPCM treated animals (2.7 ± 0.3%) when compared to both control animals (0.7 ± 0.2%, P=0.043) and the ECM+EPC group (1.7 ± 0.3%, P=0.049), as depicted in Figure 6A. Qualitative assessment of photomicrogrpahs from control (Figure 6B) and experimental (Figure 6C) borderzone myocardial sections revealed a more densely packed, organized capillary network in the treated group. These data correlate with the increase in vessel density that was noted with PECAM/α-SMA vascular labeling.

Adverse Ventricular Remodeling Is Diminished Following EPCM Treatment

Infarct area and infarct fraction were significantly smaller in EPCM animals (Area: 3.27 ± 0.35 mm^2; Fraction: 7.08 ± 0.57%) when compared to controls (Area: 8.64 ± 0.87 mm^2, P=0.004; Fraction: 15.76 ± 1.09%, P=0.002). Comparisons of EPCM versus other groups showed significantly smaller infarct sizes as well (Figure 7A). A marked increase in borderzone wall thickness was also observed in the EPCM group (EPCM: 1.41 ± 0.04 mm; Control: 1.07 ± 0.08 mm; P=0.002). A significant decrease in LVID among the EPCM group was also noted (EPCM: 8.61 ± 0.07 mm; Control: 9.74 ± 0.29 mm; P=0.005). Representative sections are shown in Figure 7B (control) and 7C (experimental).

Echocardiographic Assessment Shows Improved LV Function and Geometry Following EPCM Treatment

Echocardiographic assessment of cardiac structure and function demonstrated significant benefits in the EPCM group versus the control group (Table 1). At two weeks, EPCM animals had a significantly improved ejection fraction when compared to controls (61 ± 4 % vs. 43 ± 1%, P=0.018). At four weeks, the EPCM animals again had a significantly greater ejection fraction than controls (68 ± 2% vs. 40 ± 4%, P<0.001). Among EPCM animals, LVID was smaller in both systole and diastole, while the infarct wall thickness was greater.

Invasive Hemodynamic Assessment Shows Improved LV Function Following EPCM Treatment

The EPCM animals exhibited statistically significant preservation of cardiac function compared with controls (Table 1). The EPCM group had improved maximum pressure, maximum dP/dt, and stroke work. When compared to all other groups, EPCM animals had improved contractility, indicated by an increased slope of the end systolic pressure-volume relationship. This improvement was statistically significant when compared to the control and ECM groups and trending toward significance when compared to the ECM+EPC group.

A comparison of contractility is included in Figure 8, which also depicts representative pressure-volume loops after IVC occlusion. Cardiac output as measured by direct Doppler flow was also significantly greater in the EPCM group (Table 1).

Discussion

The results of the present study indicate that the cells isolated to generate the EPCM are indeed EPCs. In vitro, they express the VEGFR2 membrane receptor and exhibit phenotypic markers consistent with EPCs. Additionally, they behave in a manner consistent with EPCs, as evidenced by migration toward the EPC chemokine SDF and formation of primitive capillary tubules in Matrigel. In vivo, we have shown that borderzone myocardium in the EPCM group has significantly upregulated levels of VEGF, indicative of an ongoing angiogenic process as late as four weeks after matrix implantation. The results also indicate that vessel density and microvascular perfusion were significantly greater in the borderzone region of EPCM animals. These findings, in conjunction with upregulated levels of VEGF, are consistent with the known vasculogenic mechanisms of EPCs, and thus are attributable to the SDF primed EPC matrix. Additionally, a comparison of borderzone TNFα levels between groups showed similar levels which indicate that the angiogenic effects are not the result of differing levels of inflammation.

We have demonstrated that EPCM therapy attenuates adverse ventricular remodeling. Animals in the treated group had smaller infarcts, thicker peri-infarct borderzone myocardium, and smaller ventricular diameters after MI. Preservation of ventricular geometry resulted in improved ventricular function as measured by three separate modalities. Echocardiography demonstrated a statistically significant increase in fractional shortening. P-V conductance catheter measurements of maximum pressure, stroke work, dPdt max, and contractility were all greater in the EPCM group, as was cardiac output measured by Doppler flow.

Our previous work has shown modest functional and angiogenic benefits of extracellular matrix therapy alone and with seeded EPCs; thus, we included a direct comparison of these additional groups to ensure the benefits of EPCM therapy are a result of the activated EPC matrix, and not the individual components. This comparison shows that EPCM is superior to the ECM patch alone, the ECM patch treated with SDF, and the ECM+EPC groups. EPCM showed markedly greater levels of borderzone VEGF at four weeks. Comparing the EPCM group with the ECM+EPC group shows statistically significant increases in vessel density and microvascular perfusion, indicating that pretreatment with SDF had a profound effect on borderzone neovasculogenesis. Consequently, the EPCM group had smaller infarcts and improved ventricular function when compared to all other groups.

We postulate that the preservation of ventricular geometry and function is the result of improved microvascular perfusion in the borderzone myocardium. Improved perfusion results in less cell death, leaving a more viable peri-infarct myocardium that is more resistant to wall stress and resultant ventricular dilation. In addition, preservation of borderzone myocardium enhances overall ventricular function.

Our group has previously investigated the effects of endogenous upregulation of EPCs as a neovasculogenic therapy for ischemic cardiomyopathy in this model.[6–7] Based on these findings, we began to explore the effects of ex vivo expanded EPCs in the same setting. Systemic and direct myocardial injection of EPCs, however, is fraught with complications such as cell dispersion and high percentages of cell death; therefore, we aimed to engineer a novel delivery mechanism that would be more applicable to human translation. Noting that most EPC culture protocols, including ours, utilize fibronectin or vitronectin as a ligand to select for EPCs, we elected to employ a decellularized porcine jejunal submucosa extracellular matrix scaffold composed mostly of these proteins. This approach enabled a straightforward construction process by which we applied the cells directly to the matrix, and they subsequently adhered to native proteins already present. Additionally, the architecture of the extracellular matrix is similar to the cells' native environment which we postulate promotes enhanced viability. In addition to the above benefits, similar extracellular fibrous sheets are already FDA approved for use as pericardial or myocardial septal patches, which streamlines the potential translation of this therapy to human studies. One can argue that a xenogenic matrix may induce a more robust inflammatory response, but we believe that the advantages stated above outweigh this disadvantage, and the data provided regarding borderzone TNFα levels supports this. For each of the above reasons, we opted to utilize an extracellular matrix scaffold as opposed to a synthetic biodegradable material, and the end result was a densely adherent cell sheet that is easily manipulated and sutured to the ventricular wall. This construct allows for the delivery of a greater number of EPCs to the ischemic area of myocardium and effectively serves as a "paracrine factory," eluting angiogenic cytokines in the exact area of interest. Given our previous work and experience with SDF, we believe that pretreatment of the EPC matrix amplifies this process. The upregulation of these angiogenic factors has two effects. First, native endothelial cells are activated and proliferate to form new vessels. Secondly, native EPCs are recruited to the ischemic area in larger numbers, enhancing the vasculogenic response and restarting the cycle of native endothelial cell proliferation.[13] In our study, this two-pronged attack clearly results in enhanced borderzone microvascular perfusion and preserved ventricular function. In addition to the above, several animals in the treated group were noted to have highly vascular pericardial adhesions at reoperation. Based on this observation, we postulate that the EPC matrix could also be facilitating the formation of additional transepicardial collaterals that contribute to the neovasculogenic process in the ischemic borderzone, further enhancing microvascular perfusion.

We believe EPCM therapy is translatable to humans. Human trials involving direct myocardial injection of endothelial progenitors are ongoing,[5] and our institution is currently conducting a Phase I trial investigating the safety of surgical implantation of human fibroblast cell sheets in areas of nonrevascularizable myocardium. It is reasonable to suggest that an EPC matrix would produce as good a clinical benefit, if not better. The major limitation of human translatability of this therapy is the difficulty in harvesting enough EPCs to generate the EPC matrix in a timely fashion.

The results of this study, while promising, do generate several unanswered questions. Despite showing increased levels of borderzone VEGF four weeks after MI, the fate of the transplanted EPCs is unknown, and although they are harvested from syngeneic animals, it

is possible that they are eliciting an immune response. Additionally, further studies are needed to determine if a dose-response relationship exists with differing quantities of transplanted EPCs.

In conclusion, our results confirm that the treatment of myocardial ischemia with an extracellular matrix scaffold seeded with EPCs primed with SDF preserves ventricular function. We have established that this activated EPC construct, via a paracrine effect, generates a profound neovasculogenic response, and the resulting enhancement of borderzone microvascular perfusion results in preservation of ventricular geometry and function.

Acknowledgments

Sources of Funding

1. NIH 1R01HL089315-01 “Angiogenic Tissue Engineering to Limit Post-Infarction Ventricular Remodeling.” (2008–2013, Total $1,968,750)
2. NIH NHLBI/Thoracic Surgery Foundation for Research and Education jointly sponsored Mentored Clinical Scientist Development Award, 1K08HL072812, “Angiogenesis and Cardiac Growth as Heart Failure Therapy.” (2004–2009, Total $1,037,310)
3. American College of Surgeons Resident Research Scholar. “Endothelial Progenitor Derived Neovasculogenesis for Myocardial Ischemia.” (2007–2009, Total $60,000)
4. NIH Training Grant, T-32-HL07843-11. “Training Program in Cardiovascular Biology and Medicine.” (2007–2009, Total $86,000)

References

1. World Health Statistics 2008. Geneva: World Health Organization; 2008.
2. van der Bogt KE, Sheikh AY, Schrepfer S, Hoyt G, Cao F, Ransohoff KJ, Swijnenburg RJ, Pearl J, Lee A, Fischbein M, Contag CH, Robbins RC, Wu JC. Comparison of different adult stem cell types for treatment of myocardial ischemia. Circulation. 2008; 118:S121–129. [PubMed: 18824743]
3. Assmus B, Schächinger V, Teupe C, Britten M, Lehmann R, Döbert N, Grünwald F, Aicher A, Urbich C, Martin H, Hoelzer D, Dimmeler S, Zeiher AM. Transplantation of Progenitor Cells and Regeneration Enhancement in Acute Myocardial Infarction (TOPCARE-AMI). Circulation. 2002; 106:3009–3017. [PubMed: 12473544]
4. Sinha S, Poh KK, Sodano D, Flanagan J, Ouilette C, Kearney M, Heyd L, Wollins J, Losordo D, Weinstein R. Safety and efficacy of peripheral blood progenitor cell mobilization and collection in patients with advanced coronary heart disease. J Clin Apher. 2006; 21:116–120. [PubMed: 16342193]
5. Losordo DW, Schatz RA, White CJ, Udelson JE, Veereshwarayya V, Durgin M, Poh KK, Weinstein R, Kearney M, Chaudhry M, Burg A, Eaton L, Heyd L, Thorne T, Shturman L, Hoffmeister P, Story K, Zak V, Dowling D, Traverse JH, Olson RE, Flanagan J, Sodano D, Murayama T, Kawamoto A, Kusano KF, Wollins J, Welt F, Shah P, Soukas P, Asahara T, Henry TD. Intramyocardial transplantation of autologous CD34+ stem cells for intractable angina: a phase I/IIa double-blind, randomized controlled trial. Circulation. 2007; 115:3165–3172. [PubMed: 17562958]
6. Asahara T, Murohara T, Sullivan A, Silver M, van der Zee R, Li T, Witzenbichler B, Schatteman G, Isner JM. Isolation of putative progenitor endothelial cells for angiogenesis. Science. 1997; 275:964–967. [PubMed: 9020076]
7. Atluri P, Liao GP, Panlilio CM, Hsu VM, Leskowitz MJ, Morine KJ, Cohen JE, Berry MF, Suarez EE, Murphy DA, Lee WM, Gardner TJ, Sweeney HL, Woo YJ. Neovasculogenic therapy to augment perfusion and preserve viability in ischemic cardiomyopathy. Ann Thorac Surg. 2006; 81:1728–1736. [PubMed: 16631663]

8. Woo YJ, Grand TJ, Berry MF, Atluri P, Moise MA, Hsu VM, Cohen J, Fisher O, Burdick J, Taylor M, Zentko S, Liao G, Smith M, Kolakowski S, Jayasankar V, Gardner TJ, Sweeney HL. Stromal cell-derived factor and granulocyte-monocyte colony-stimulating factor form a combined neovasculogenic therapy for ischemic cardiomyopathy. J Thorac Cardiovasc Surg. 2005; 130:321–329. [PubMed: 16077394]
9. Kocher AA, Schuster MD, Szabolcs MJ, Takuma S, Burkhoff D, Wang J, Homma S, Edwards NM, Itescu S. Neovascularization of ischemic myocardium by human bone-marrow-derived angioblasts prevents cardiomyocyte apoptosis, reduces remodeling and improves cardiac function. Nat Med. 2001; 7:430–436. [PubMed: 11283669]
10. Asahara T, Masuda H, Takahashi T, Kalka C, Pastore C, Silver M, Kearne M, Magner M, Isner JM. Bone marrow origin of endothelial progenitor cells responsible for postnatal vasculogenesis in physiological and pathological neovascularization. Circ Res. 1999; 85:221–228. [PubMed: 10436164]
11. Zemani F, Silvestre JS, Fauvel-Lafeve F, Bruel A, Vilar J, Bieche I, Laurendeau I, Galy-Fauroux I, Fischer AM, Boisson-Vidal C. Ex vivo priming of endothelial progenitor cells with SDF-1 before transplantation could increase their proangiogenic potential. Arterioscler Thromb Vasc Biol. 2008; 28:644–650. [PubMed: 18239152]
12. Murasawa S, Llevadot J, Silver M, Isner JM, Losordo DW, Asahara T. Constitutive human telomerase reverse transcriptase expression enhances regenerative properties of endothelial progenitor cells. Circulation. 2002; 106:1133–1139. [PubMed: 12196341]
13. Urbich C, Aicher A, Heeschen C, Dernbach E, Hofmann WK, Zeiher AM, Dimmeler S. Soluble factors released by endothelial progenitor cells promote migration of endothelial cells and cardiac resident progenitor cells. J Mol Cell Cardiol. 2005; 39:733–742. [PubMed: 16199052]
14. Ii M, Nishimura H, Iwakura A, Wecker A, Eaton E, Asahara T, Losordo DW. Endothelial progenitor cells are rapidly recruited to myocardium and mediate protective effect of ischemic preconditioning via “imported” nitric oxide synthase activity. Circulation. 2005; 111:1114–1120. [PubMed: 15723985]
15. Sellke FW, Li J, Stamler A, Lopez JJ, Thomas KA, Simons M. Angiogenesis induced by acidic fibroblast growth factor as an alternative method of revascularization for chronic myocardial ischemia. Surgery. 1996; 120:182–188. [PubMed: 8751581]
16. Takeshita S, Zheng LP, Brogi E, Kearney M, Pu LQ, Bunting S, Ferrara N, Symes JF, Isner JM. Therapeutic angiogenesis. A single intraarterial bolus of vascular endothelial growth factor augments revascularization in a rabbit ischemic hind limb model. J Clin Invest. 1994; 93:662–670. [PubMed: 7509344]
17. Yin L, Morishige K, Takahashi T, Hashimoto K, Ogata S, Tsutsumi S, Takata K, Ohta T, Kawagoe J, Takahashi K, Kurachi H. Fasudil inhibits vascular endothelial growth factor-induced angiogenesis in vitro and in vivo. Mol Cancer Ther. 2007; 6:1517–1525. [PubMed: 17513600]
18. Frederick, JR.; Fitzpatrick, JR.; McCormick, RC.; Harris, DA.; Kim, AY.; Muenzer, JR.; Smith, MJ.; Cohen, JE.; Atluri, P.; Woo, YJ. Tissue Engineered Endothelial Progenitor Cell Construct Promotes Neovasculogenesis, Enhances Perfusion, and Improves Ventricular Function after Myocardial Infarction. American College of Surgeons 95th Annual Clinical Congress; October 11–15, 2009; Abstract
19. Frederick, JR.; Fitzpatrick, JR.; McCormick, RC.; Harris, DA.; Kim, A.; Smith, MJ.; Laporte, CM.; Muenzer, JR.; Gambogi, AJ.; Woo, YJ. Extracellular Matrix Scaffold Restores Ventricular Function by Attenuating Adverse Ventricular Remodeling after Myocardial Infarction. American College of Cardiology 58th Annual Scientific Session; March 29–31, 2009; Abstract
20. Sekine H, Shimizu T, Hobo K, Sekiya S, Yang J, Yamato M, Kurosawa H, Kobayashi E, Okano T. Endothelial cell coculture within tissue-engineered cardiomyocyte sheets enhances neovascularization and improves cardiac function of ischemic hearts. Circulation. 2008; 118:S145–152. [PubMed: 18824746]
21. Pacher P, Nagayama T, Mukhopadhyay P, Bátkai S, Kass DA. Measurement of cardiac function using pressure-volume conductance catheter technique in mice and rats. Nat Protoc. 2008; 3:1422–1434. [PubMed: 18772869]

22. Liu YH, Yang XP, Nass O, Sabbah HN, Peterson E, Carretero OA. Chronic heart failure induced by coronary artery ligation in Lewis inbred rats. Am J Physiol. 1997; 272:H722–727. [PubMed: 9124430]

23. Woo YJ, Panlilio CM, Cheng RK, Liao GP, Suarez EE, Atluri P, Chaudhry HW. Myocardial regeneration therapy for ischemic cardiomyopathy with cyclin A2. J Thorac Cardiovasc Surg. 2007; 133:927–933. [PubMed: 17382628]

24. Gee MS, Procopio WN, Makonnen S, Feldman MD, Yeilding NM, Lee WM. Tumor vessel development and maturation impose limits on the effectiveness of anti-vascular therapy. Am J Pathol. 2003; 162:183–193. [PubMed: 12507901]

25. Brown L, Fenning A, Chan V, Loch D, Wilson K, Anderson B, Burstow D. Echocardiographic assessment of cardiac structure and function in rats. Heart Lung Circ. 2002; 11:167–73. [PubMed: 16352093]

Figure 1A

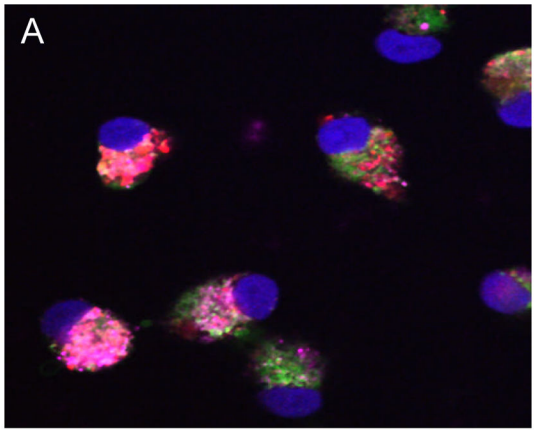

Figure 1B&C

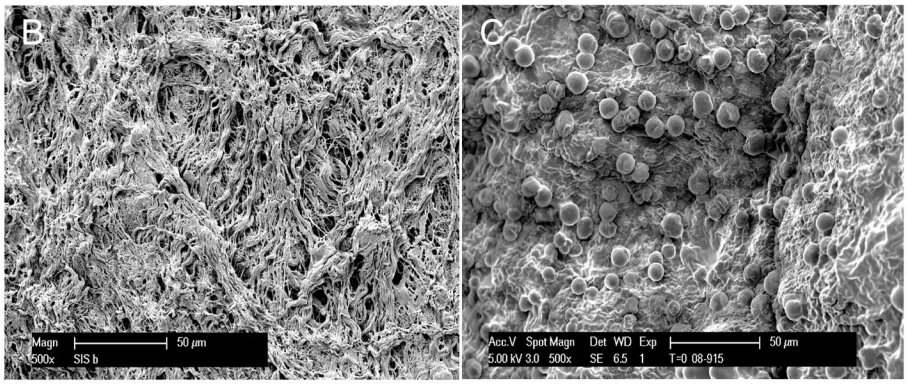

Figure 1.

Figure 1A- At day seven in culture, isolated MNCs grown on extracellular matrix show universal expression of VEGFR2 (pink), stain positive for Isolectin (green), and show uptake of Di-Iodinated acetyl-LDL (red), all of which are characteristic of EPCs (nuclei are stained with DAPI-blue).

Figure 1B&C- Scanning electron micrographs of ECM before (B) and after (C) seeding with EPCs show densely populated, adherent cells

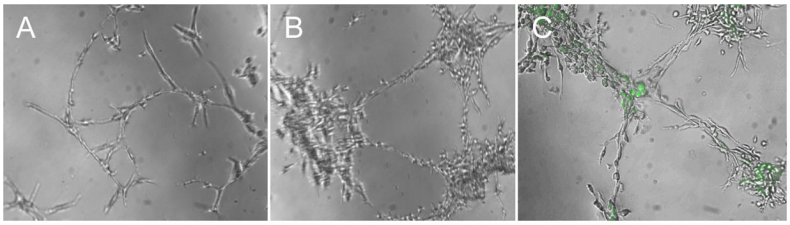

Figure 2.

Figure 2A,B&C. Utilizing the Matrigel tube formation assay, isolated cells show progressive sprout and tubule formation at 24 (A), 48 (B), and 72 hours (C) and stain positive with Calcein AM (green), a viability marker.

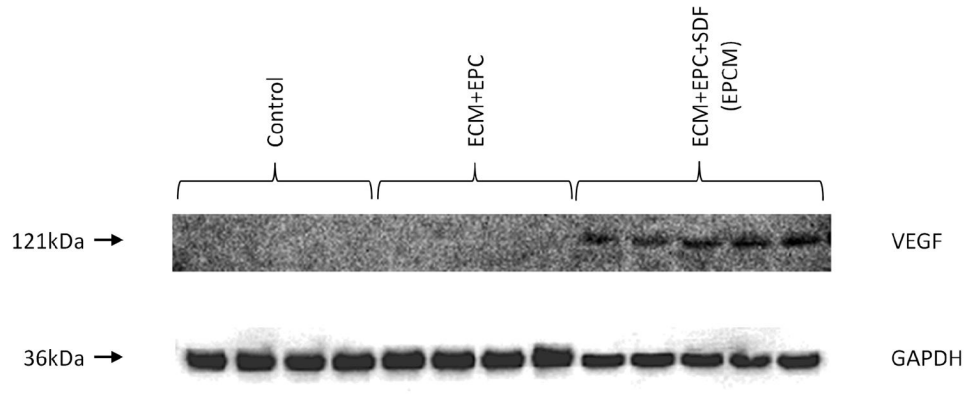

Figure 3.

At four weeks, borderzone myocardial tissue samples show significantly increased levels of rat VEGF in the EPCM group versus the control and ECM+EPC groups. Glyceraldehyde 3-phosphate dehydrogenase (GAPDH) staining was performed to demonstrate equivalent protein loading between lanes.

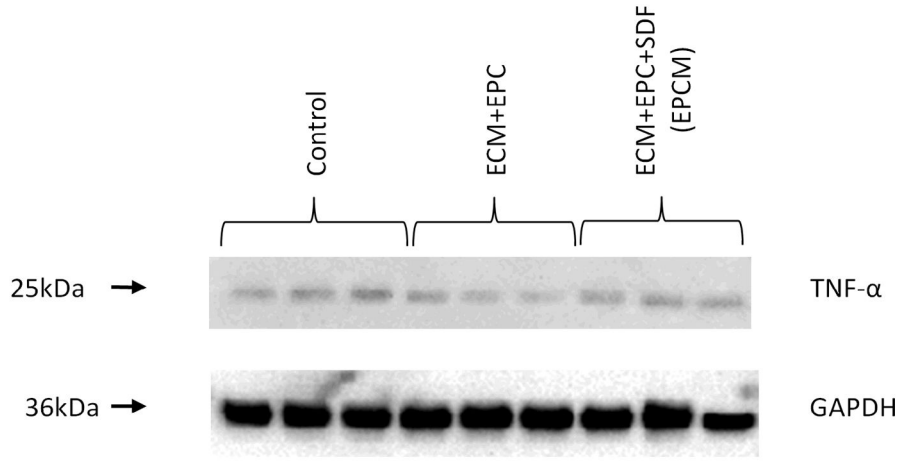

Figure 4.

At four weeks, immunoblotting of borderzone myocardial tissue samples revealed similar levels of TNFα between the control, ECM+EPC, and EPCM groups. Glyceraldehyde 3-phosphate dehydrogenase (GAPDH) staining was performed to demonstrate equivalent protein loading between lanes.

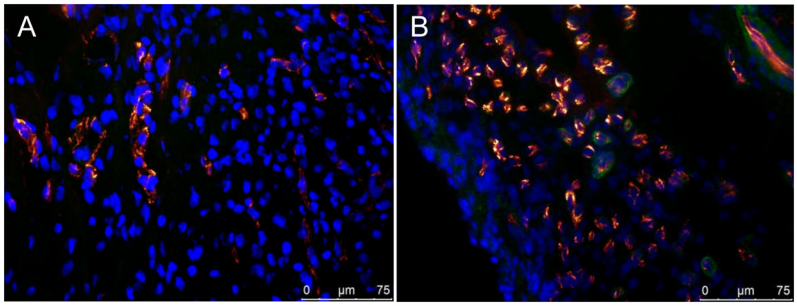

Figure 5.

Figure 5A&B- Analysis of immunofluorescent co-expression of PECAM (orange) and α-SMA (green) revealed a significant increase in blood vessel density in the borderzone region of EPCM animals. Quantitative analysis of vessel density shows 4.1 ± 0.3 vessels/HPF in the control group compared to 6.2 ± 0.3 vessels/HPF in the EPCM group, $P<0.001$. Representative photomicrographs of control (A) and EPCM treated animals (B) are shown.

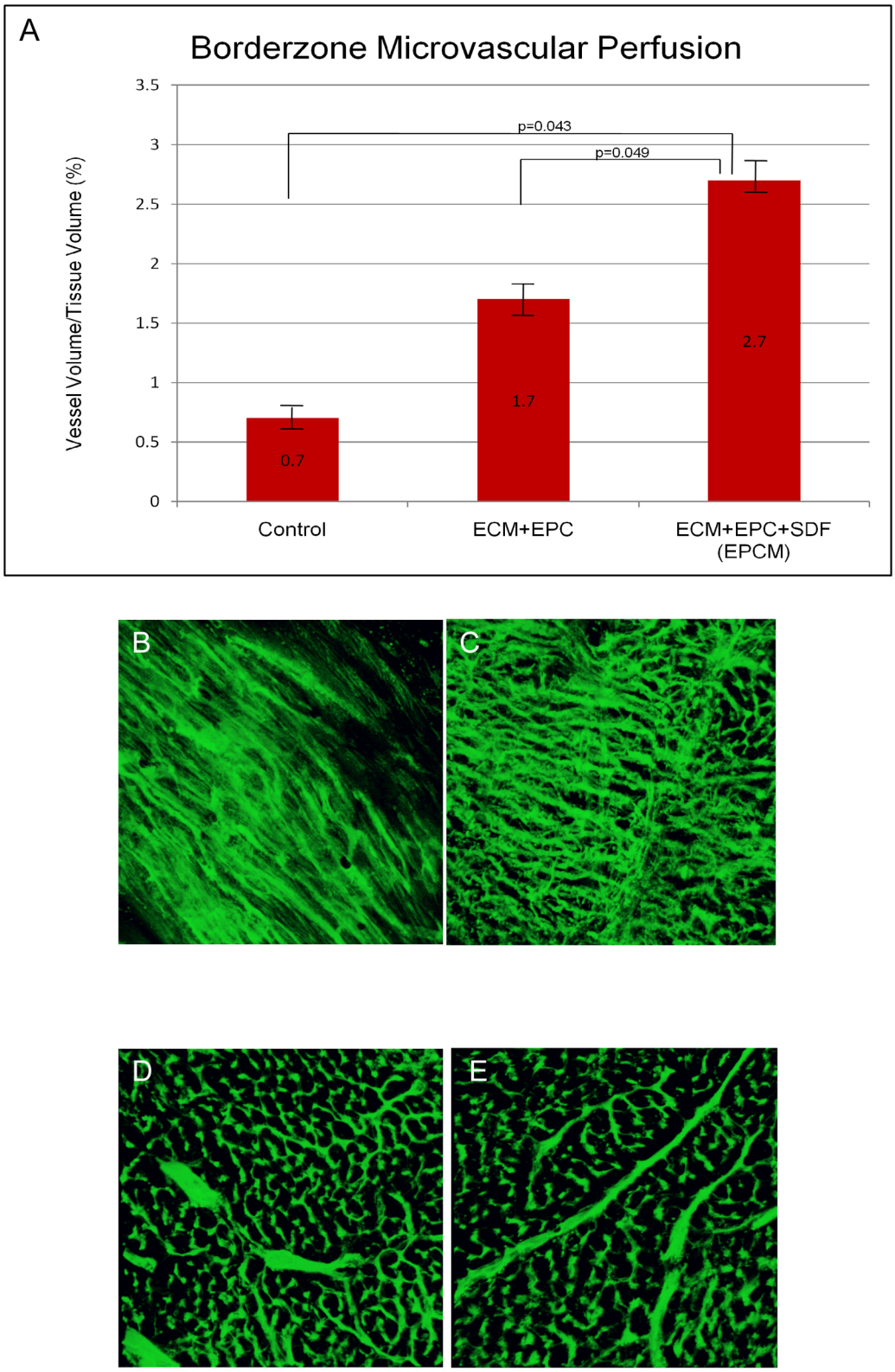

Figure 6.

Figure 6A,B&C- Quantitative analysis of lectin microangiography demonstrated significantly enhanced perfusion in the borderzone region of EPCM treated animals (2.7 ± 0.3%) when compared to both control animals (0.7 ± 0.2%, P=0.043) and the ECM+EPC group (1.7 ± 0.3%, P=0.049), as depicted in Figure 6A. Qualitative assessment of photomicrogrpahs from control (Figure 6B) and EPCM (Figure 6C) borderzone myocardial sections revealed a more densely packed, organized capillary network in the treated group. Remote myocardial sections from control (Figure 6D) and EPCM animals (Figure 6E) are included for comparison.

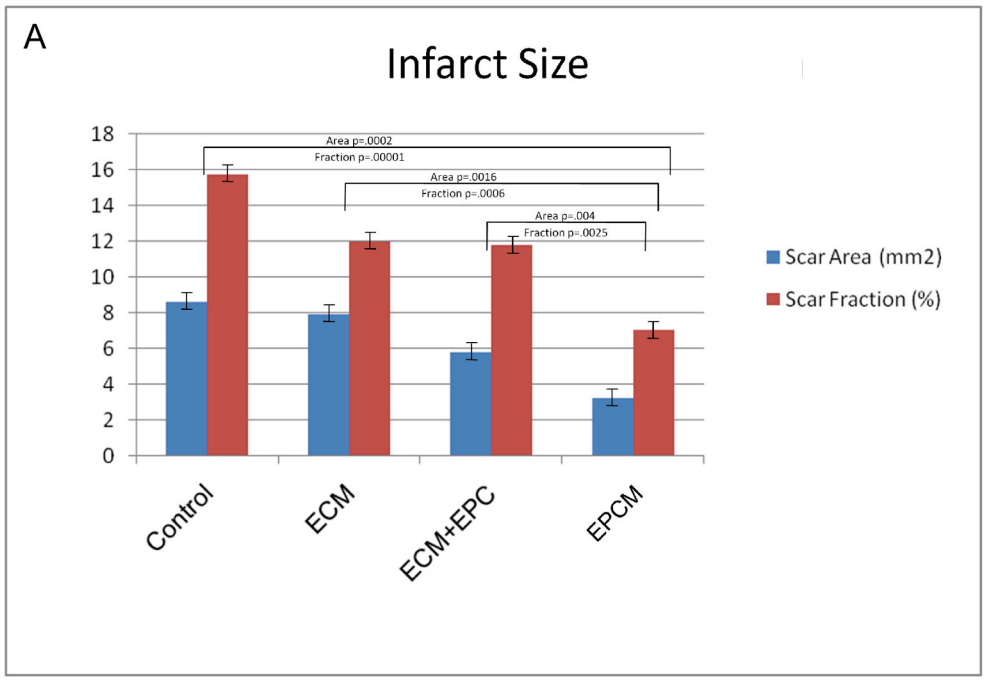

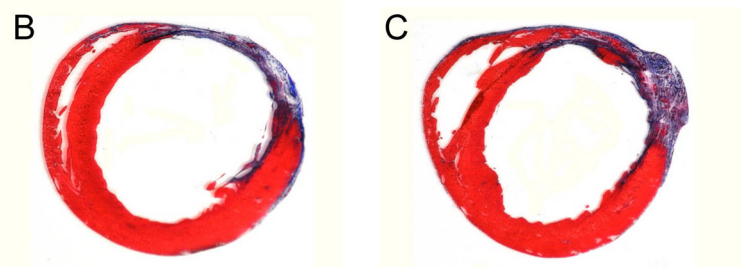

Figure 7.

Figure 7A,B&C - Infarct area and infarct fraction were significantly smaller in EPCM animals (Area: 3.27 ± 0.35 mm^2; Fraction: 7.08 ± 0.57%) versus controls (Area: 8.64 ± 0.87 mm^2, P=0.004; Fraction: 15.76 ± 1.09%, P=0.002). Comparisons of EPCM versus other groups showed significantly smaller infarct sizes as well (A). Representative sections of a control (B) and an EPCM (C) treated animal depicting reduced infarct size, increased borderzone thickness, and preserved ventricular geometry of the EPCM treated animal are shown for comparison.

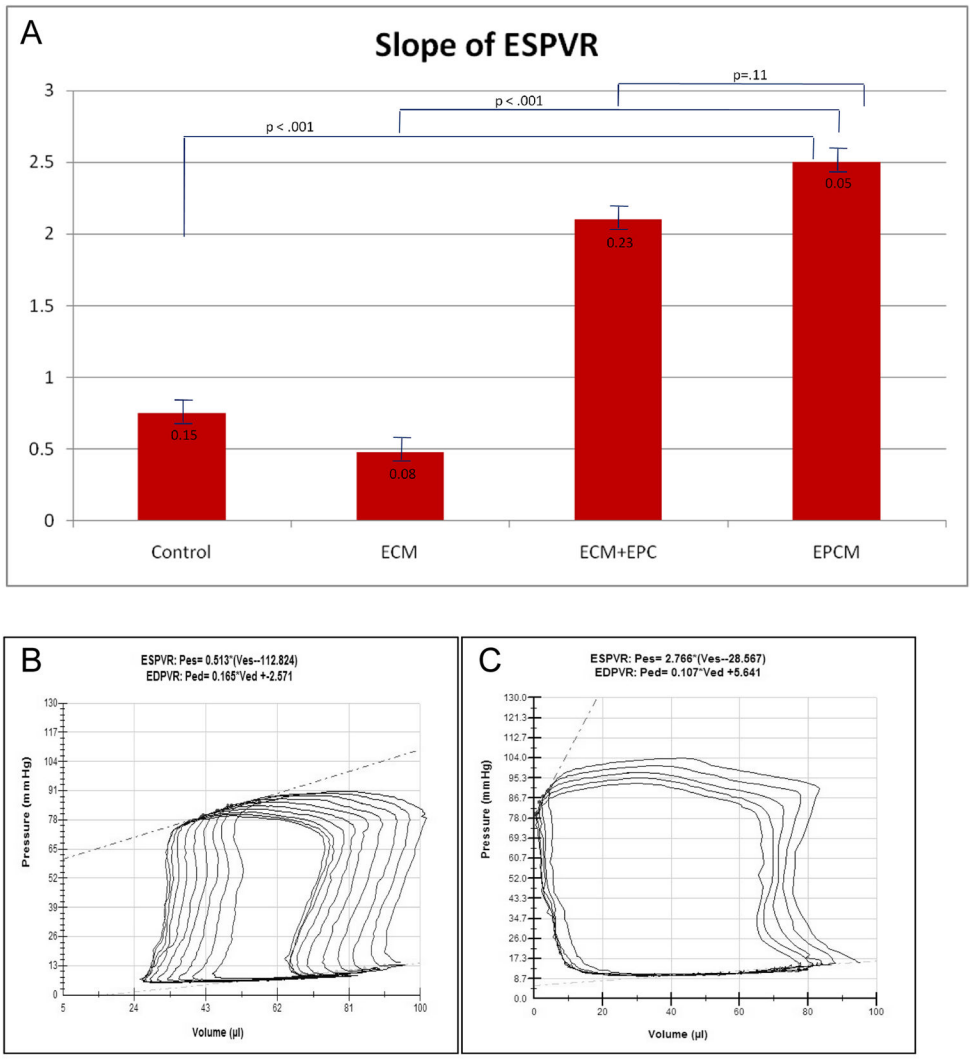

Figure 8.

Figure 8A,B&C- A comparison of contractility expressed as the slope of ESPVR (A). Representative P-V loops during IVC occlusion from a control (B) and an EPCM (C) treated animal depict a higher maximum pressure, a greater ejection fraction, and markedly better contractility in the treated group.

Table 1

At four weeks, left ventricular function was preserved after EPCM treatment as measured by echocardiography, pressure-volume conductance catheter, and Doppler flow.

Modality	Parameter	Control (n=22)	EPCM (n=21)	P Value
Echo	LVID systole (mm)	0.67 ± 0.02	0.45 ± 0.02	<0.001
	LVID diastole (mm)	0.80 ± 0.02	0.66 ± 0.01	0.001
	Infarct Wall Thickness diastole (mm)	1.13 ± 0.11	1.70 ± 0.10	<0.001
	Infarct Wall Thickness systole (mm)	1.20 ± 0.12	1.96 ± 0.06	<0.001
	Fractional Shortening (%)	16 ± 2	32 ± 1	<0.001
	Ejection Fraction (%)	40 ± 4	68 ± 2	<0.001
P-V Conductance	Maximum Pressure (mmHg)	95.7 ± 2.5	118.3 ± 5.1	<0.001
	dPdt Max (mmHg/sec)	4237 ± 293	5927 ± 388	<0.001
	Stroke Work (mmHg*uL)	3998 ± 440	5464 ± 642	0.006
	Slope of end systolic pressure-volume relationship	0.75 ± 0.15	2.50 ± 0.05	<0.001
Doppler Flow	Cardiac Output (ml/min)	27.3 ± 3.4	39.8 ± 1.1	0.029